Rate constants for CN reactions with hydrocarbons and the product HCN vibrational populations: Examples of heavy–light–heavy abstraction reactions

Leon R. Copeland, Fida Mohammad, Mansour Zahedi, David H. Volman, and William M. Jackson

Citation: The Journal of Chemical Physics **96**, 5817 (1992); doi: 10.1063/1.462681
View online: http://dx.doi.org/10.1063/1.462681
View Table of Contents: http://scitation.aip.org/content/aip/journal/jcp/96/8?ver=pdfcov
Published by the AIP Publishing

Articles you may be interested in

Quantum mechanical elucidation of reaction mechanisms of heavy-light-heavy systems: Role of potential ridge
J. Chem. Phys. **108**, 8922 (1998); 10.1063/1.476338

Erratum: Rate constants for CN reactions with hydrocarbons and the product HCN vibrational populations: Examples of heavy–light–heavy abstraction reactions [J. Chem. Phys. 96, 5817 (1992)]
J. Chem. Phys. **97**, 3878 (1992); 10.1063/1.463994

Adiabatic separatrix crossing theory for heavy–light–heavy chemical reactions in three dimensions
J. Chem. Phys. **95**, 7234 (1991); 10.1063/1.461401

Energy distribution of the CN products of the H+HCN, H+ClCN, and F+HCN reactions
J. Chem. Phys. **90**, 7096 (1989); 10.1063/1.456238

Oscillating reactivity of collinear symmetric heavy+light–heavy atom reactions
J. Chem. Phys. **78**, 3850 (1983); 10.1063/1.445162

This article is copyrighted as indicated in the article. Reuse of AIP content is subject to the terms at: http://scitation.aip.org/termsconditions. Downloaded to IP: 130.216.129.208 On: Wed, 17 Dec 2014 02:40:12

Rate constants for CN reactions with hydrocarbons and the product HCN vibrational populations: Examples of heavy–light–heavy abstraction reactions

Leon R. Copeland, Fida Mohammad, Mansour Zahedi, David H. Volman, and William M. Jackson
Department of Chemistry, University of California, Davis, California 95616

(Received 15 August 1991; accepted 10 January 1992)

The rate constants for the reactions of CN radicals with methane, ethane, propane, cyclopropane, isobutane, and neopentane have been measured over a temperature range from 275 to 455 K. Laser photolysis was used to produce the radicals and time delayed laser induced fluorescence was used to follow the radical concentration as a function of time. The temperature dependence of the observed rate constants could be fitted with a three-parameter Arrhenius plot. The activation energies that were observed were all small and in some cases they were negative. Time resolved ir emission was used to follow the formation of the HCN($0n2$) and HCN($0n'1$) product emission. The time dependence of the relative emission intensities, as well as computer modeling of the decay curves, suggest that vibrational population inversion occurs for all of the hydrocarbons studied except methane and cyclopropane. These observations are discussed in terms of the current theories for these type of reactions.

INTRODUCTION

Earlier we have described room temperature measurements of the rate constants for the reactions of CN radicals with hydrocarbons.[1,2] In those experiments the rate constants were found to be very large, approaching those of ion molecule reactions for propane, butane, and neo-pentane. It was postulated that this was because of attractive forces in the entrance channel of the reaction which lead to "complex" formation. Complex formation is understood to mean any interaction that increases the interaction time so that it is longer than the nominal time for the CN reactant to pass by the target molecule. This includes consideration of an interaction distance greater than that predicted on the basis of a hard sphere interaction. To further investigate this phenomenon we decided to determine the Arrhenius parameters for a number of these reactions. We also wanted to see if we could identify the major product of the reaction which was presumed to be HCN.

EXPERIMENTAL

A block diagram of the experimental apparatus used to measure the rate constants is given in Fig. 1. The laser beams enter the cell via suprasil quartz windows mounted on baffle arms and propagate through the cell in opposite directions. The photolysis source was either a low intensity Math Sciences Northwest ArF laser with a maximum energy per pulse of 1 mJ at 193 nm and a pulse width of 5 ns or a Lambda Physik EMJ 103 ArF Laser with a pulse energy of 1 mJ/pulse and a pulse width of 20 ns. The concentration of CN radicals produced by these lasers is about 2×10^{12} cm^{-3}, assuming an absorption coefficient for C_2N_2 of 2×10^{-19} cm^2 and a quantum yield of two. This is considerably less than the concentrations of the reactants used in these studies assuring that the measurements will be done under pseudo-first-order conditions.

The probe source is a Molectron (UV-12) nitrogen laser pumped (DL-II) dye laser utilizing an (Exciton) BBQ dye. This laser generates narrow bandwidth (0.7 cm^{-1}) tunable light which covers the range of the CN($B\,^2\Sigma \leftarrow X\,^2\Sigma$) transition operating with a repetition rate of 10 Hz and a pulse width of 10 ns.

The concentration of the CN radicals was measured by monitoring with the dye laser the $P_{00}(8)$ line for CN($v''=0$) and $R_{11}(8)$ line for CN($v''=1$) of the $B\,^2\Sigma \leftarrow X\,^2\Sigma$. Pseudo-first-order decay constants were obtained by determining the intensity of one of the above rota-

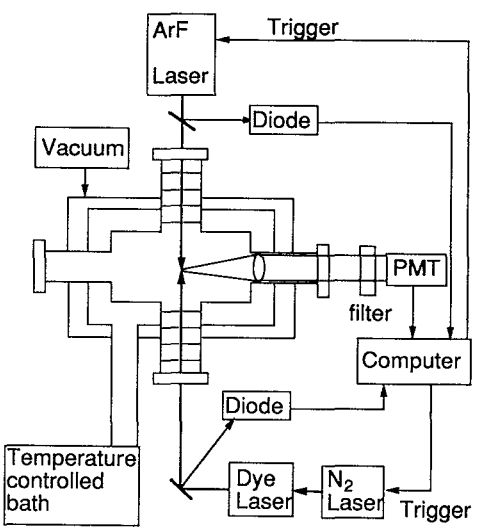

FIG. 1. Schematic diagram of the laser induced fluorescence apparatus that was used for determining the rate constants for the CN + RH reactions.

This article is copyrighted as indicated in the article. Reuse of AIP content is subject to the terms at: http://scitation.aip.org/termsconditions. Downloaded to IP: 130.216.129.208 On: Wed, 17 Dec 2014 02:40:12

 0021-9606/92/085817-10$06.00 © 1992 American Institute of Physics

tional lines as a function of delay time between both lasers. The fluorescence signal was collected perpendicular to the laser beams by a 1 in. diameter, 2 in. focal length quartz lens, and passed through a bandpass filter and focused onto the cathode of a photomultiplier tube (Thorn-EMI 9789QB). The signal from this PM tube goes into a Stanford Research SR250 boxcar integrator connected to a Laser Interface LI-1000 series control and data acquisition system. After a preset number of shots the computer increased the delay time and the signal was measured. The intensities of both lasers were also determined on a shot by shot basis, stored in the computer and used to normalize the measured signals.

The temperature of the cell was controlled by passing Dow Corning 200 fluid between the cell walls with a Neslab EX-250HT high temperature bath. This bath is capable of producing temperatures up to 250 °C with a stability of about 0.02 °C. Using a Neslab EN-Flow through cooler (EN-350), temperatures down to about − 15 °C with a stability of about 0.01 °C may be obtained with a 50:50 mixture of ethylene glycol and water as the bath liquid. An Omega type T thermocouple, placed less than 1 cm above the reaction zone, was used to monitor the temperature inside the cell with an accuracy of 1 °C.

The delays and timing were also controlled with an IBM PC compatible computer fitted with a Laser Interface LI-1100 interface board coupled to a LI-1200 external interface system. The computer was set to obtain several data points at different delay times between the ArF laser pulse, which produces the CN radicals and the dye laser which detects them. These pulses are provided by programmable timers which are crystal controlled with less than 2 ns jitter and an incremental resolution of 100 ns per step. Each data point was averaged over 200 laser shots before it was stored in the computer.

Pseudo-first-order rate constants were obtained at different pressures of the reactant gas, and were then plotted vs concentration of the reactant gas. The true rate coefficient was obtained from the slope of the resulting plot. This process was repeated at different temperatures and the data fitted to a three-parameter Arrhenius equation of the type

$$k = AT^n \exp(-E/\mathrm{RT}). \quad (1)$$

Separate mixtures of reactant gas, C_2N_2 and argon were made up in five 2 ℓ flasks and allowed to equilibrate overnight. This mixture was slowly flowed through the reactor at a total pressure for most experiments of 20 Torr. The C_2N_2 partial pressure in the reaction cell was 50 mTorr, while the pressure of reactant gas varied from 14 to 792 mTorr depending on which gas was used. The total pressure inside the cell was measured with a calibrated capacitance manometer (MKS Baratron model 222B). The C_2N_2 (Matheson, 98.5% min), methane (Matheson, 99.99% min), ethane (Matheson, 99.99% min), and propane (Matheson, 99.98% min) were purified by degassing several times at

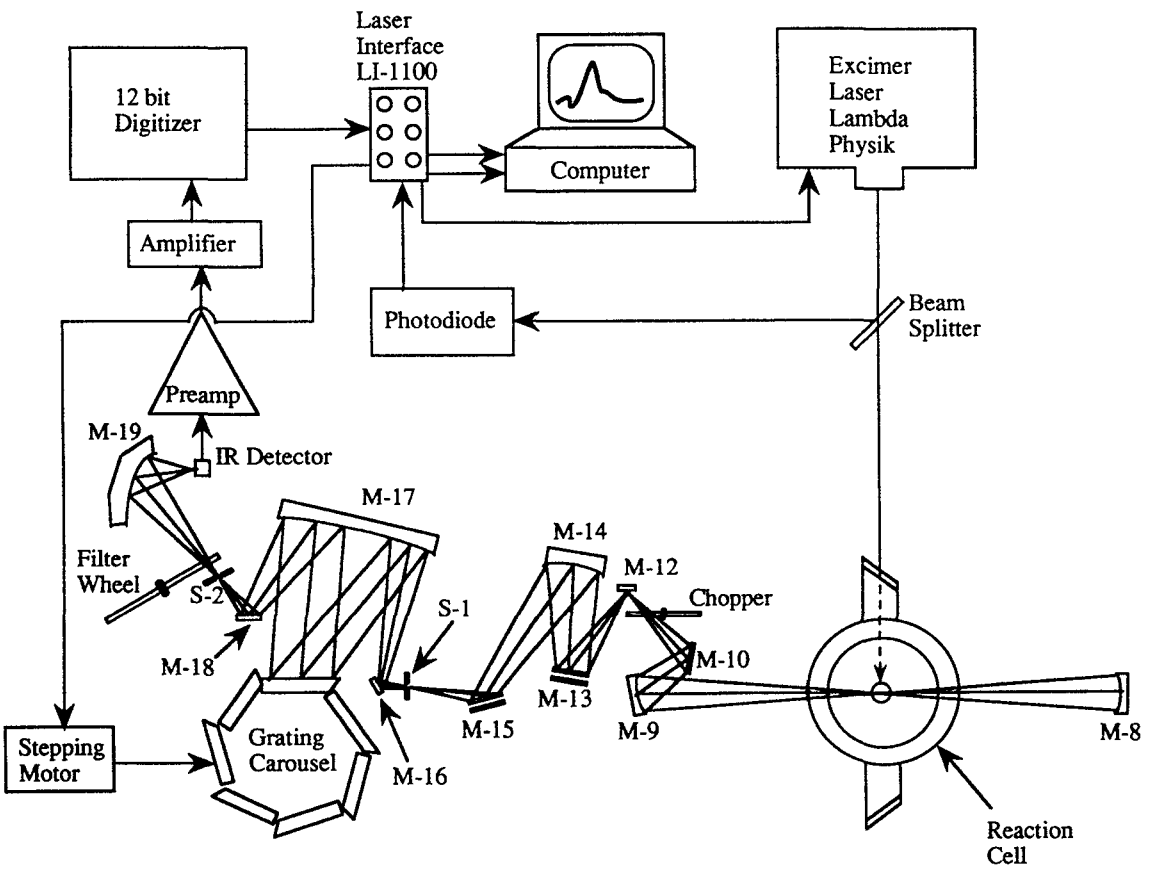

FIG. 2. Schematic diagram of the time resolved infrared fluorescence apparatus that was used for determining the infrared emission from vibrationally excited HCN formed in the CN + RH reactions.

This article is copyrighted as indicated in the article. Reuse of AIP content is subject to the terms at: http://scitation.aip.org/termsconditions. Downloaded to IP: 130.216.129.208 On: Wed, 17 Dec 2014 02:40:12

liquid N_2 temperatures. After they were added to the storage vessel, argon (Spectra Gases Inc., 99.999%) was added at the proper pressure without further purification.

The block diagram of the apparatus used for the time resolved infrared experiments is shown in Fig. 2. An unfocused Lambda Physik EMG 103 ArF excimer laser with an output energy from 40–50 mJ per pulse passed through a quartz window into the reaction cell. The size of the excimer laser beam was 3.2×1.2 cm^2 so the fluence was between 10 and 13 mJ/cm^2. This laser photolyzes C_2N_2, producing CN radicals which react with the hydrocarbon that is present inside the cell. Argon is added to the cell to reduce diffusion to the walls and to purge the entrance and exit windows. Infrared emission that occurs in the cell is picked up by mirrors M-9 and M-8 and focused onto the slit S-1 of the Perkin–Elmer Model 180 ir monochromator. This light is dispersed by the appropriate grating, passed through an order sorting filter, and focused onto a fast Santa Barbara Associates liquid N_2 cooled detector. It then goes sequentially to a preamplifier, an amplifier, and a Laser Interface 12 bit, 1 μs transient digitizer. The output of the digitizer is interfaced with a computer using the same type of interface unit that was used for the rate constant measurements. The frequency of the laser is set to 28 Hz and synchronized to a chopper wheel. Background measurements are made when the chopper wheel blocks the direct emission from the reaction cell on alternate laser shots. The transient signal is stored in the computer and the data is typically averaged for 1000 laser shots. After the emission signal has been averaged, the computer steps the monochromator to the next infrared wavelength and the process is repeated. The intensity of the photolysis laser is also stored and used to correct each signal for fluctuations of the photolysis laser. Spectra as a function of delay time can then be obtained by sorting all of this data to obtain a matrix of intensity as a function of wavelength and delay time.

RESULTS AND DISCUSSION

Kinetic measurements

A typical example of the decay curves that have been obtained in these studies is shown in Fig. 3 for the reaction of CN with CH_4 at a pressure of 792 mTorr and a temperature of 280 K. The decay constants measured from curves of this type are then corrected for both the residual reaction with C_2N_2 and diffusion. These corrections are measured in separate experiments using C_2N_2 and argon under conditions that are otherwise identical to those with the reactant gas. The corrected pseudo-first-order rate constants derived from these decay constants are then plotted as a function of the methane number density. An example of such a plot is given in Fig. 4. The error bars associated with the experimental points is the one sigma standard deviation for the corrected decay rate constants. If no error bar is reported the error was below the size of the points. The line going through the points is a least squares fit to data using the point at zero pressure as part of the fit. The slopes of these curves is then the first order rate constant for reactions of the type

$$CN + RH \rightarrow \text{Products}. \quad (1)$$

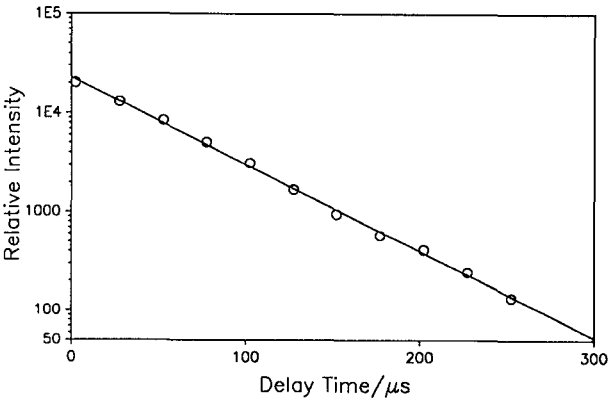

FIG. 3. A plot of a typical decay curve for CN reacting with methane at a pressure of 0.792 Torr and a temperature of 280 K. The one sigma standard deviation are reported, and if no error bars are given the error is smaller than the size of the points.

Figures 5(a) through 5(e) are "Arrhenius"-type plots of the rate constants measured in this study. Table I summarizes all of the rate constants with the rate expressions that gave the best fit to the temperature plots. Only methane and cyclopropane show the "classical Arrhenius" behavior, where the temperature dependent rate constant can be fitted with a two-parameter Arrhenius plot, i.e., an A factor and an activation energy E, where the rate constant increases with increasing temperature. A three-parameter fit is needed to fit all of the other temperature dependent rate constants to an Arrhenius type of plot. Even when this is done for propane and neopentane the activation energies associated with these plots are negative. Previously Tulley and his colleagues suggested that for propane this was due to the competition between abstraction of a primary and a secondary hydrogen atom.[10] The fact that even neopentane, which has only primary hydrogens, exhibits the same behavior is proof that this can not be the explanation for the negative activation energies in these molecules since there are no secondary hydrogens. Lin and his co-workers have also observed a negative activation energy for the reaction of CN radicals with pro-

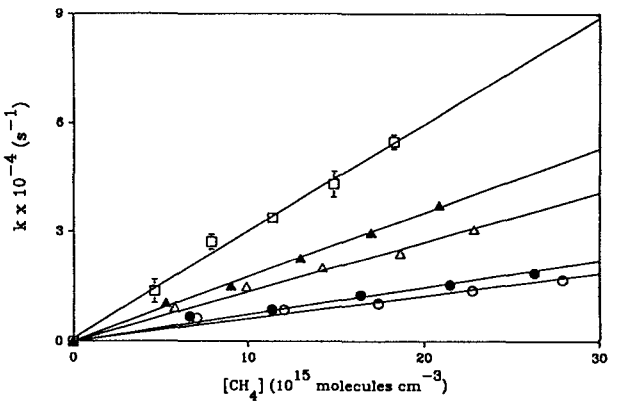

FIG. 4. Pseudo-first-order rate constant vs concentration of methane. The one sigma standard deviation are reported, and if no error bars are given the error is smaller than the size of the points. ○, ●, △, ▲, and □ for temperatures 280, 297, 342, 375, and 428 K.

This article is copyrighted as indicated in the article. Reuse of AIP content is subject to the terms at: http://scitation.aip.org/termsconditions. Downloaded to IP: 130.216.129.208 On: Wed, 17 Dec 2014 02:40:12

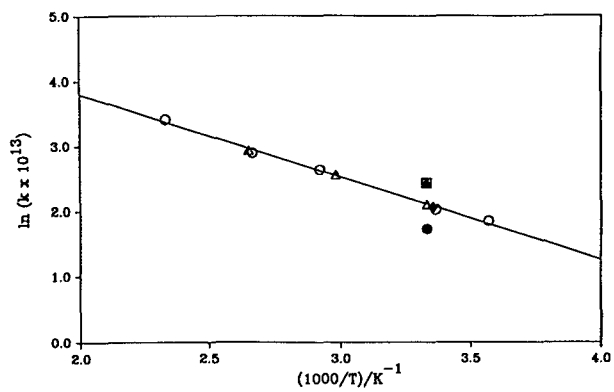

(a)

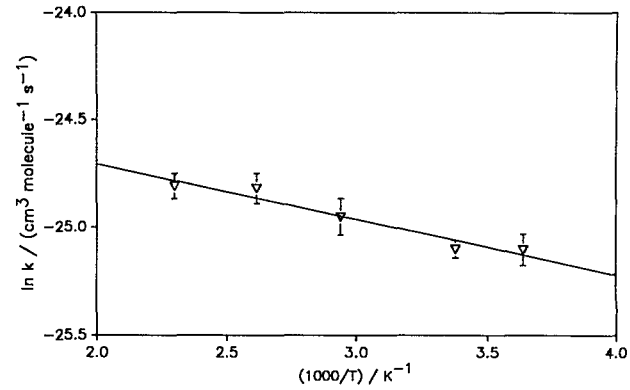

(d)

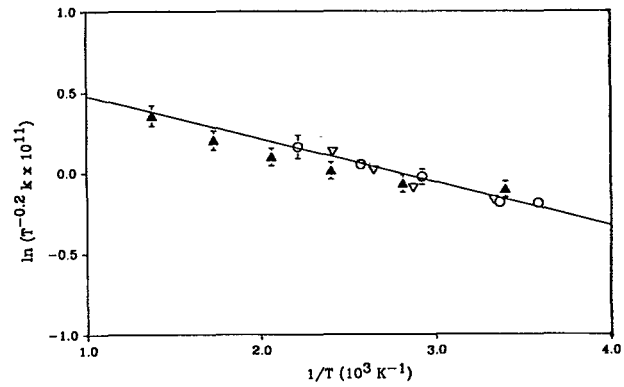

(b)

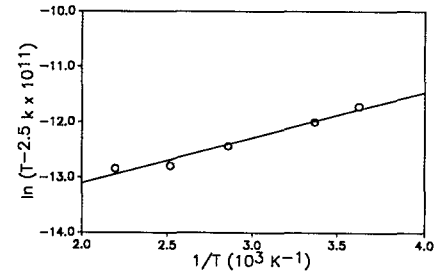

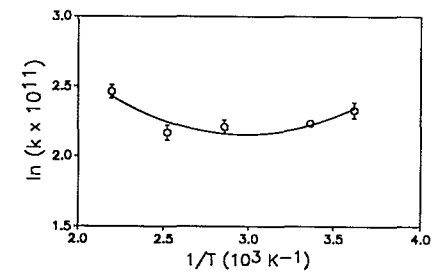

(e)

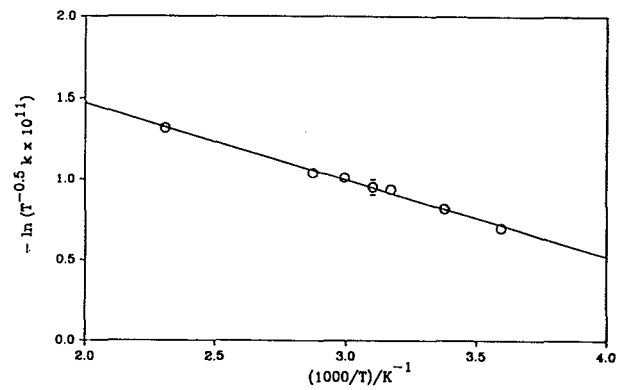

(c)

FIG. 5. (a) Arrhenius plot of the reaction of CN with methane. ○ this work; Δ Ref. 3; ● Ref. 4; ◆ Ref. 5; ▲ Ref. 6; □ Ref. 7. The one sigma standard deviation are reported, and if no error bars are given the error is smaller than the size of points. The solid line is a theoretical fit to the curve using the equation in Table I. (b) Arrhenius plots of the reaction of CN with ethane. ○ this work; ▽ Ref. 8; ▲ Ref. 9. The one sigma standard deviation are reported, and if no error bars are given the error is smaller than the size of points. The solid line is a theoretical fit to the curve using the equation in Table I. (c) Arrhenius plots of the reaction of CN with propane. The one sigma standard deviation are reported, and if no error bars are given the error is smaller than the size of the points. The solid line is a theoretical fit to the curve using the equation in Table I. (d) Arrhenius plots of the reaction of CN with cyclopropane. The one sigma standard deviation are reported, and if no error bars are given the error is smaller than the size of the points. The solid line is a theoretical fit to the curve using the equation in Table I. (e) Arrhenius plots of the reaction of CN with neopentane. The one sigma standard deviation are reported, and if no error bars are given the error is smaller than the size of the points. The solid line in the top plot is a theoretical fit to the curve using the equation in Table I. The bottom graph is the standard two parameter Arrhenius plot which shows the curvature.

This article is copyrighted as indicated in the article. Reuse of AIP content is subject to the terms at: http://scitation.aip.org/termsconditions. Downloaded to IP: 130.216.129.208 On: Wed, 17 Dec 2014 02:40:12

TABLE I. Summary of the measured rate constants.[a]

Temp (K)	k (cm^3 molecule^{-1} s^{-1})
$CN + CH_4$	
280	$6.3 \pm 0.4 \times 10^{-13}$
297	$7.5 \pm 0.6 \times 10^{-13}$
342	$1.4 \pm 0.6 \times 10^{-12}$
375	$1.8 \pm 0.2 \times 10^{-12}$
428	$3.0 \pm 0.2 \times 10^{-12}$
$k(T) = 5.6 \pm 0.1 \times 10^{-11} \exp[-1.7 \pm 0.6/RT]$ (cm^3 molecule^{-1} s^{-1})	
$CN + C_2H_6$	
279	$2.5 \pm 0.2 \times 10^{-11}$
297	$2.6 \pm 0.2 \times 10^{-11}$
342	$3.1 \pm 0.4 \times 10^{-11}$
389	$3.5 \pm 0.2 \times 10^{-11}$
452	$4.0 \pm 0.6 \times 10^{-11}$
$k(T) = 2.1 \pm 1.0 \times 10^{-11} T^{0.2} \exp[-0.6 \pm 0.3/RT]$ (cm^3 molecule^{-1} s^{-1})	
$CN + C_3H_8$	
279	$8.3 \pm 0.2 \times 10^{-11}$
297	$7.6 \pm 0.2 \times 10^{-11}$
315	$7.0 \pm 0.6 \times 10^{-11}$
322	$6.9 \pm 0.6 \times 10^{-11}$
334	$6.7 \pm 0.4 \times 10^{-11}$
348	$6.6 \pm 0.4 \times 10^{-11}$
433	$5.6 \pm 0.4 \times 10^{-11}$
$k(T) = 9.1 \pm 0.10 \times 10^{-13} T^{0.5} \exp[0.9 \pm 0.1/RT]$ (cm^3 molecule^{-1} s^{-1})	
$CN + C(CH_3)_4$	
276	$1.0 \pm 0.1 \times 10^{-10}$
297	$9.3 \pm 0.2 \times 10^{-11}$
350	$9.1 \pm 0.5 \times 10^{-11}$
397	$8.7 \pm 0.5 \times 10^{-11}$
455	$1.2 \pm 0.1 \times 10^{-11}$
$k(T) = 4.2 \pm 0.30 \times 10^{-18} T^{2.5} \exp[1.6 \pm 0.1/RT]$ (cm^3 molecule^{-1} s^{-1})	
$CN + c\text{-}C_3H_6$	
275	$1.3 \pm 0.1 \times 10^{-11}$
296	$1.3 \pm 0.1 \times 10^{-11}$
340	$1.5 \pm 0.2 \times 10^{-11}$
382	$1.6 \pm 0.2 \times 10^{-11}$
435	$1.7 \pm 0.1 \times 10^{-11}$
$k(T) = 3.1 \pm 0.20 \times 10^{-11} \exp[-0.5 \pm 0.1/RT]$ (cm^3 molecule^{-1} s^{-1})	

[a] All of the errors are quoted as $\pm 2\sigma$ and E is in kcal/mol.

pane, and with isobutane.[7] Thus there are now several laboratories that suggest that small negative activation energies are associated with the abstraction of a H atom from the larger saturated hydrocarbons.

Negative activation energies are usually associated with complex formation during the course of a reaction. They have previously been observed for radical–radical reactions, radical–addition, and, more recently, for the reactions of alkyl radicals with Br_2.[11–13] The common characteristic in all of these reactions is the exothermicity associated with the reaction. However, in the first two examples a new bond is formed which should aid in the formation of a transient complex. In the present experiments and in the case of the alkyl reactions with bromine, a true addition reaction can not be occurring since Br_2 and the alkanes have completely saturated valences. Rather than a true addition reaction in this case, we suggest that the long range attractive forces lead to a "loose complex" which increases the magnitude of the collision rate constant. This general idea is supported by our earlier work which showed that there was a correlation between the magnitude of the classical attractive forces and the magnitude of the room temperature rate constants.

Product state distributions are often a good clue to the lifetime of transition states since long lived states should lead to a statistical distribution of the final products. On the other hand, if population inversion in the vibrational or rotational distributions of the products is observed, it is a good indication that the interaction does not last long enough for randomization to occur. In the next section time resolved infrared emission studies will be described and the results will be discussed in terms of the rate constants measurements.

It is generally assumed that the main product of the reaction of CN with saturated hydrocarbons is HCN, but the only evidence that supports this are studies with hydrogen and methane.[5] Even in this case, where HCN was detected in ir absorption from the ground vibrational level, a signal was only observed after many collisions, implying that the HCN is formed with a considerable amount of internal energy. The exothermicity of the abstraction reaction is large enough in all of these systems so that vibrationally excited HCN molecules can be produced. Since this is a heavy–light–heavy system we should, by analogy with other such systems, expect to see vibrational excitation in the HCN if it is formed in the reaction. The apparatus shown in Fig. 2 was used to determine if vibrationally excited HCN is produced in the reaction. All of the reactions were studied at room temperature with a mixture of hydrocarbon, cyanogen, and argon gases in the ratio 1:10:50. Photolysis of cyanogen at 193 nm produces only CN($X\,^2\Sigma^+$) radicals with 75% in the $v'' = 0$ and 25% in the $v'' = 1$ levels.[14] Jackson *et al.* have shown that, with tne exception of methane, the vibrational energy of the CN fragment does not enhance the rate of these reactions.[1]

Decay curves at $\nu = 3340$ and 3170 cm^{-1} that were obtained using propane as a reactant are shown in Fig. 6. It is an example of the strong HCN emission signals that were

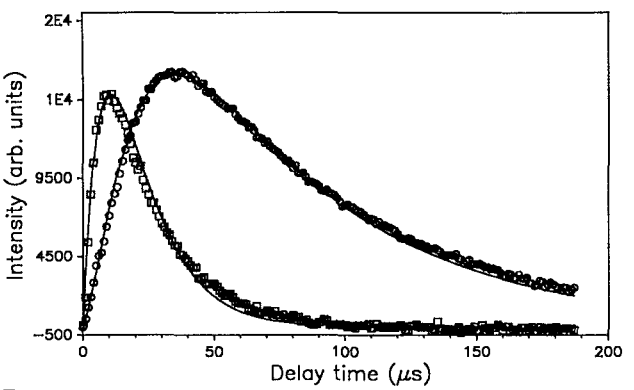

FIG. 6. Transient infrared fluorescent decay curves at 3340 cm^{-1} (slow) and at 3170 cm^{-1} (fast) obtained in the reaction of CN radicals with C_3H_8. The solid line is a theoretical fit to the curve using the model described in the text.

This article is copyrighted as indicated in the article. Reuse of AIP content is subject to the terms at: http://scitation.aip.org/termsconditions. Downloaded to IP: 130.216.129.208 On: Wed, 17 Dec 2014 02:40:12

observed with all of the hydrocarbons. The transient infrared signal obtained in these experiments consists of a series of time decay curves taken with the infrared monochromator set at different wavelengths. Reasonable signal-to-noise ratios were obtained by averaging the transient signals over 1000 laser shots. After the scan was completed and all of the data stored in the computer it was then sorted into spectra at a given delay time and plotted as a function of frequency. The resulting spectra are reported in Figs. 7(a) to 7(h). The resolution of these spectra is not high enough to resolve individual rotational lines but the band origin for the ν_3 (001) → (000) at 3311 cm^{-1} is clearly visible. The spectra also show emission in the region of the ν_3 (002) → (001) at 3207 cm^{-1}. All of the emission spectra should be rotationally relaxed because the total pressure in the system ranges from 3–6 Torr, which means that the number of collisions that a molecule undergoes in an observation time of 1 μs varies from 30 to 60 collisions. The peak intensity of the R branch of the HCN(001) → HCN(000) transition is at $J'' = 8$ at long delay times, which is where it should be for a Boltzmann distribution with a temperature of 300 K. At short delay times only H_2, CH_4, and c-C_3H_8 show maximum rotational intensity at this point. It is unlikely at these pressures that the HCN is not always rotationally equilibrated, so it must be concluded that vibrational excitation is responsible for this behavior. The three molecules, i.e., H_2, CH_4, and c-C_3H_8, that show well developed rotationally equilibrated bands are also the molecules which have the

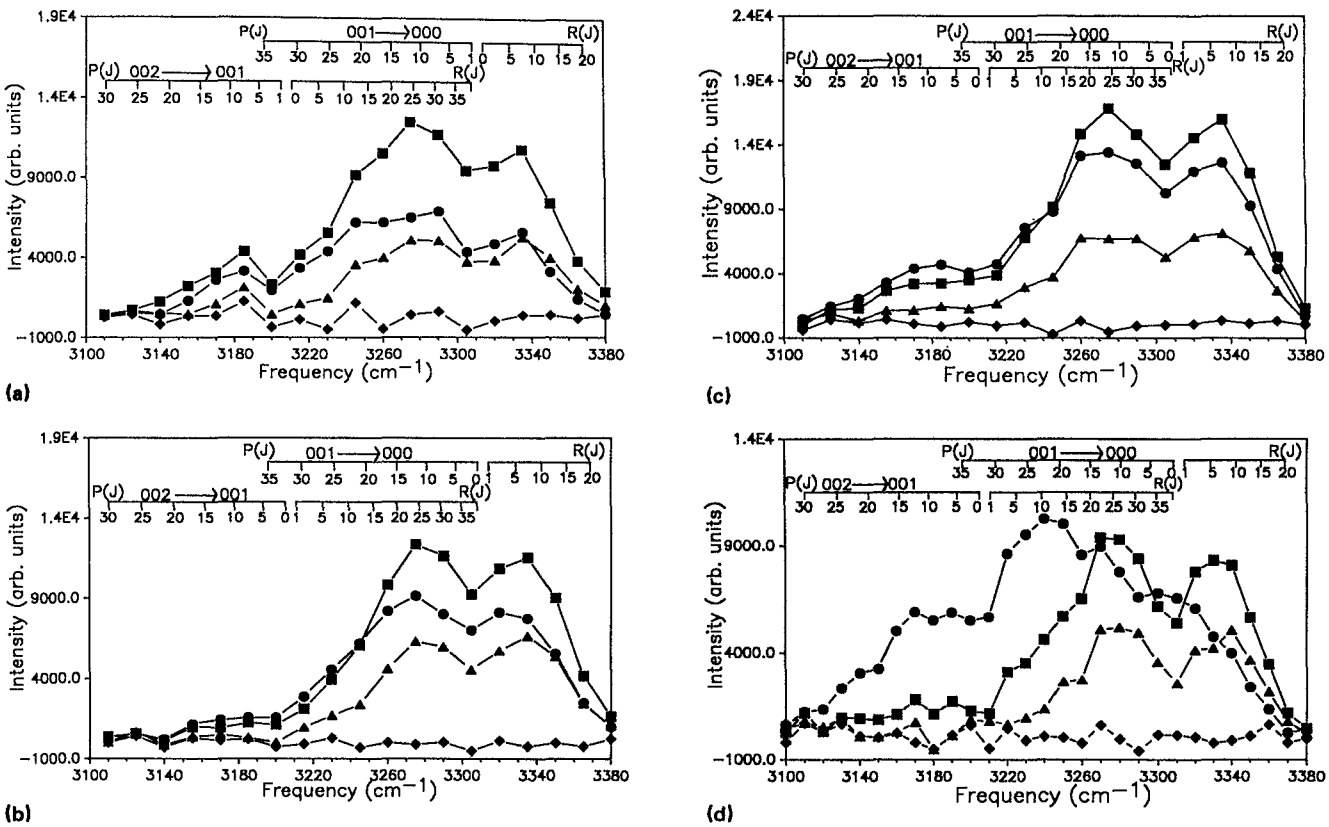

FIG. 7. (a) Time resolved emission spectra for the reaction of CN radicals with CH_4. The ◆, ●, ■, and ▲ are for reaction times of 0, 10, 23, and 110 μs, respectively. The P_{CH_4}, $P_{C_2N_2}$, and P_{Ar} are 0.37, 1.48, and 3.37 Torr, respectively. The slit width is 4.5 mm slit width for an approximate resolution of 22.5 cm^{-1}. (b) Time resolved emission spectra for the reaction of CN radicals with c-C_3H_6. The ◆, ●, ■, and ▲ are for reaction times of 0, 15, 35, and 110 μs, respectively. The $P_{c\text{-}C_3H_6}$, $P_{C_2N_2}$, and P_{Ar} are 0.060, 0.600, and 1.32 Torr, respectively. The slit width is 4.5 mm slit width for an approximate resolution of 22.5 cm^{-1}. (c) Time resolved emission spectra for the reaction of CN radicals with H_2. The ◆, ●, ■, and ▲ are for reaction times of 0, 50, 100, and 350 μs, respectively. The P_{H_2} and $P_{C_2N_2}$ are 1.73 and 1.59 Torr. The slit width is 5 mm slit width for an approximate resolution of 25 cm^{-1}. (d) Time resolved emission spectra for the reaction of CN radicals with C_2H_6. The ◆, ●, ■, and ▲ are for reaction times of 0, 15, 61, and 105 μs, respectively. The slit width is 3.0 mm slit width for an approximate resolution of 15 cm^{-1}. (e) Time resolved emission spectra for the reaction of CN radicals with C_3H_8. The ◆, ●, ■, and ▲ are for reaction times of 0, 16, 21, and 61 μs, respectively. The $P_{C_3H_8}$, $P_{C_2N_2}$, and P_{Ar} are 0.100, 1.45, and 8.43 Torr, respectively. The slit width is 3.0 mm slit width for an approximate resolution of 15 cm^{-1}. (f) Time resolved emission spectra for the reaction of CN radicals with n-C_4H_{10}. The ◆, ●, ■, and ▲ are for reaction times of 0, 6, 18, and 68 μs, respectively. The $P_{n\text{-}C_4H_{10}}$, $P_{C_2N_2}$, and P_{Ar} are 0.127, 0.926, and 3.94 Torr, respectively. The slit width is 4.5 mm slit width for an approximate resolution of 22.5 cm^{-1}. (g) Time resolved emission spectra for the reaction of CN radicals with $C(CH_3)_4$. The ◆, ●, ■, and ▲ are for reaction times of 0, 3, 7, and 70 μs, respectively. The $P_{C(CH_3)_4}$, $P_{C_2N_2}$, and P_{Ar} are 0.110, 0.600, and 1.28 Torr, respectively. The slit width is 4.5 mm slit width for an approximate resolution of 22.5 cm^{-1}. (h) Time resolved emission spectra for the reaction of CN radicals with i-C_4H_{10}. The ◆, ●, ■, and ▲ are for reaction times of 0, 6, 18, and 100 μs, respectively. The $P_{i\text{-}C_4H_{10}}$, $P_{C_2N_2}$, and P_{Ar} are 0.179, 0.969, and 3.99 Torr, respectively. The slit width is 4.5 mm slit width for an approximate resolution of 22.5 cm^{-1}.

This article is copyrighted as indicated in the article. Reuse of AIP content is subject to the terms at: http://scitation.aip.org/termsconditions. Downloaded to IP: 130.216.129.208 On: Wed, 17 Dec 2014 02:40:12

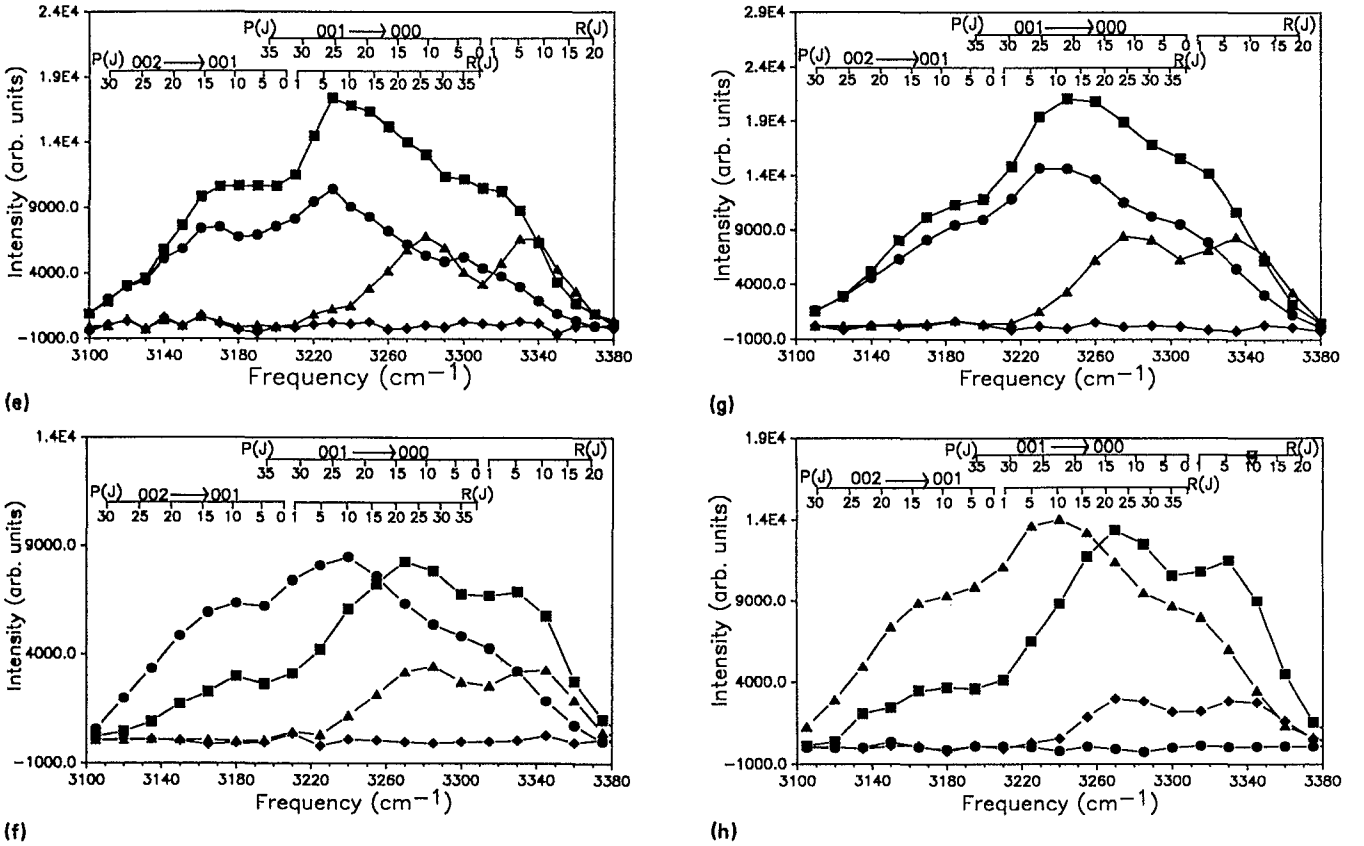

FIG. 7. (*Continued.*)

lowest exothermicity. This suggests that they should also have the lowest population of HCN(002) molecules formed in the reaction.

The spectra for the other molecules with higher exothermicities all show very little HCN(001), at short delay times, as evidenced by the small population in the R branch. Since this R branch is not overlapped by contributions from the R branch of the rotationally equilibrated HCN(002) level the spectra strongly suggest that more HCN(002) is produced in the reaction than HCN(001) for these molecules.

Two methods have been used to determine the relative population of HCN(002) to HCN(001) that is produced in the initial reaction. The first method sums the integrated intensity of the R branch from $J=12$ to $J=20$ for HCN(001) and divides it by the sum of the integrated intensities of the P branch of HCN(002) over the same rotational levels. This ratio is then plotted as a function of time and the extrapolated value of the intensities at zero time is determined. This ratio is related to the relative population, i.e., N_1/N_2, at zero time by the following equation:

$$\sum I^R/\sum I^P = (\alpha_1^R/\alpha_2^P)\times(F_1/F_2)\times(B_1/B_2)\times N_1/N_2, \tag{2}$$

where Σ is from $J=12$ to $J=20$, α_1^R/α_2^P is the instrumental calibration factors $=1.1$, F_1/F_2 is the relative transition probabilities, and B_1/B_2 is the Boltzmann factors, i.e.,

$$B_1/B_2 = \left[\sum S_{RJ}\exp - BJ(J+1)/k_bT\right] \Big/ \left[\sum S_{PJ}\exp - BJ(J+1)/k_bT\right].$$

The relative transition probabilities were taken from Maricq *et al.* and it is 0.55.[15] The Boltzmann factors were calculated using the line strengths, S_{RJ} and S_{PJ}, given by Herzberg and was found to be 1.1.[16] The instrumental factor was measured using the glowbar that is part of the Perkin–Elmer 180 instrument.

The relative population of the vibrationally excited HCN(002) to HCN(001) can also be determined by using a kinetic model to fit the time resolved infrared emission curve at the appropriate wavelength. The following chemical reactions are assumed to describe the kinetic behavior of the reactants and products in the system:

$$\mathrm{CN}(v''=0) + \mathrm{RH} \rightarrow \mathrm{HCN}(001) + \mathrm{R}, \tag{3}$$

$$\mathrm{CN}(v''=0) + \mathrm{RH} \rightarrow \mathrm{HCN}(002) + \mathrm{R}, \tag{4}$$

$$\mathrm{HCN}\ (001) + \mathrm{M} \rightarrow \mathrm{HCN}(000) + \mathrm{M}, \tag{5}$$

$$\mathrm{HCN}(002)\ + \mathrm{M} \rightarrow \mathrm{HCN}(001) + \mathrm{M}. \tag{6}$$

The validity of this mechanism will be tested by the theoretical fit to the experimental data and by comparison of the rate constants derived from the fit with other experimental data.

The above mechanism leads to the following set of integrated rate equations for the time dependent concentration for HCN(002) and HCN(001):

This article is copyrighted as indicated in the article. Reuse of AIP content is subject to the terms at: http://scitation.aip.org/termsconditions. Downloaded to IP: 130.[illegible] On: Sat, 20 Dec 2014 12

$$[\mathrm{HCN}(002)] = \{k_4[\mathrm{CN}]_0/(k_6 - k)\}\{\exp(-k[\mathrm{C_3H_8}]t) - \exp(-k_6[\mathrm{M}]t)\} \quad (7)$$

and

$$[\mathrm{HCN}(001)] = [\{k_3/k_4\}\{1/(k_5 - k)\}\{\exp(-k[\mathrm{C_3H_8}]t) - \exp(-k_5[\mathrm{M}]t)\} + \{k_6/[(k_6 - k)(k_5 - k)]\}\{\exp(-k[\mathrm{C_3H_8}]t) - \exp(-k_5[\mathrm{M}]t)\} - \{k_6/[(k_6 - k)(k_5 - k_6)]\}\{\exp(-k_6[\mathrm{M}]t) - \exp(-k_5[\mathrm{M}]t)\}] \times k_4[\mathrm{CN}]_0 . \quad (8)$$

An estimate of the relaxation rate for the HCN(002) is first found by computing when the total rate of formation of the vibrationally excited HCN is 86% complete. The intensity of the signal at that point is used as the starting point for measuring the decay constant k_6 for the relaxation rate. This decay constant is then used as one of the parameters in the fit. The other rate constant k is then adjusted to give the best overall visual fit to the decay curves as shown for C_3H_8 in Fig. 6. Similarly, k_5 is obtained from the decay of the tail end of the HCN(001) time resolved ir emission curve. Once k, k_5, and k_6 have been determined using the above method, these rate constants are substituted in Eq. (8) to determine the ratio of k_3/k_4 adjusting it to obtain the best overall visual fit to the transient emission curve for HCN(001). The final fits were all reasonable and similar to the fits shown in Fig. 6.

An additional check on the kinetic model is to use the k values determined from the fits and compare them with the k values determined by measuring the loss of CN radical described earlier. This comparison is given in Table II. Both the LIF method for determining the rate constants for the total loss of CN radicals, $k_{\mathrm{CN\ loss}}$ and the time resolved ir emission, $k_{\mathrm{ir\ emission}}$ give similar values for the rate constant. The present results are also in agreement with our previous results where there are overlapping measurements. There is only one major discrepancy in the table, namely, between the rate constant k_5 for quenching of HCN(001) by ethane and the rate constant for the same quenching reaction measured by Smith *et al.*[17] The present rate constant for this reaction is too fast by a factor of 4.6. This may be because our measurement is not as direct as the Smith measurement, or it may be because we are measuring the vibrational quenching rate for the HCN(011) state. The resolution of our spectrometer is not high enough to resolve the difference between the (001) and the (011) states. Experiments are currently being planned to use a cold gas HCN filter to distinguish between these two states.

Smith *et al.* have also reported the quenching rate constant for the (011) state of HCN.[17] They find that this rate constant is 4.0×10^{-12} cm^3 s^{-1}, which is much closer to the quenching rate constant of 4.5×10^{-12} cm^3 s^{-1} we have assigned to the HCN(001) state. This observation along with the observation of weak ir emission that peaks at 3975 cm^{-1}, which is about where one should expect the overtone emission for HCN(011), suggest that ir emission is probably due to the HCN(0n2) and HCN(0n'1). The intensity of the emission is about an order of magnitude less than the emission intensity at 3311 cm^{-1}, but this is to be expected since the transition probability of the combination band is expected to be at least an order of magnitude less than a fundamental band.

A byproduct of the kinetic measurements is the determination of the ratio of k_3 and k_4, the rate constants that we have assigned to the formation of HCN(001) and HCN(002), respectively. Based upon the above discussion

TABLE II. Comparison of rate constants determined by LIF and TRIRE studies.

Gas	Total rate constant		Vibrational quenching		Reference
	$k_{\mathrm{CN\ loss}}$ (cm^3/s^{-1})	$k_{\mathrm{ir\ emission}}$ (cm^3/s^{-1})	k_6 (cm^3/s^{-1})	k_5 (cm^3/s^{-1})	
CH_4				6.2×10^{-13}	
				8.5×10^{-13}	17
C_2H_6	2.7×10^{-11}				18
	2.3×10^{-11}				4
	2.4×10^{-11}				This work (LIF)
		2.6×10^{-11}	1.9×10^{-11}	4.5×10^{-12}	This work (TRIRE)
				9.8×10^{-13}	17
C_3H_8	8.1×10^{-11}				4
	7.2×10^{-11}				This work (LIF)
	7.5×10^{-11}				18
		7.6×10^{-11}	3.5×10^{-11}	7.5×10^{-12}	This work (TRIRE)
n-C_4H_{10}		9.0×10^{-11}	1.6×10^{-11}	4.2×10^{-12}	This work (TRIRE)
i-C_4H_{10}	1.0×10^{-10}				18
		8.9×10^{-11}	1.6×10^{-11}	3.7×10^{-12}	This work (TRIRE)
					This work (LIF)
$C(CH_3)_4$	0.96×10^{-10}				
		1.1×10^{-10}	4.6×10^{-11}	1.3×10^{-11}	This work (TRIRE)

This article is copyrighted as indicated in the article. Reuse of AIP content is subject to the terms at: http://scitation.aip.org/termsconditions. Downloaded to IP: 130.216.129.208 On: Wed, 17 Dec 2014 02:40:12

TABLE III. Relative populations of HCN(0*n*2)/HCN(0*n*'1) derived from kinetic and intensity measurements.

Gas	Intensity measurements $[I_{0n'1}/I_{0n2}](t=0)$[a]	Intensity measurements $[0n'1]/[0n2]$[b]	Intensity measurements %HCN(0*n*2)	Kinetic measurements $k_3/k_4 = [0n'1]/[0n2]$	Kinetic measurements %HCN(0*n*2)
CH_4	1.3	2.0	33	n.a.[c]	n.a.
C_2H_6	0.15	0.23	81	0.30	77
C_3H_8	0.15	0.23	81	0.21	83
n-C_4H_{10}	0.42	0.66	60	0.20	83
i-C_4H_{10}	0.40	0.62	62	0.10	91
neo-C_5H_{12}	0.50	0.78	56	0.29	78
c-C_3H_6	1.6	2.5	29	n.a.	n.a.
H_2	0.86	1.3	43	n.a.	n.a.

[a] $[I_{0n'1}/I_{0n2}](t=0)$ = the relative intensity in the HCN(0*n*'1) and HCN(0*n*2) spectral regions extrapolated to zero time.
[b] $[0n'1]/[0n2]$ = relative initial concentrations of [HCN(0*n*'1)]/[HCN(0*n*2)].
[c] n.a. = not applicable because kinetic analysis could not be done.

these rate constants must now be assigned to HCN(0*n*'1) and HCN(0*n*2), respectively. The assignment does not invalidate the kinetic treatment nor the determination of the relative intensities of the emission at zero reaction time. These two measurements are independent determinations of the relative concentrations of these two species. Table III summarizes these measurements for all of the gases from which we have seen ir transient emission and it also contains the results of the kinetic measurements for the relative production of HCN(0*n*'1) and HCN(0*n*2). There is reasonable agreement between the two measurements for ethane and propane, but for the higher hydrocarbons the kinetic measurements consistently yield higher HCN(0*n*2) concentrations than the intensity measurements. This could be because even at the short times, collisions have affected the relative intensities of the HCN emissions and the kinetic model is better suited to take into account these collisions.

The spectrum in Fig. 8 shows that infrared emission from the vibrationally excited HNC, the geometric isomer of hydrogen cyanide, is also present in the system. These peaks are much less intense than the HCN peaks and the slit width used in these experiments was larger than that used for detecting HCN. The overall intensity of this HNC is approximately 1% of the emission observed from HCN. The frequency of the transition is at 3630 cm^{-1}, which is the frequency of the HNC(011)→HNC(010) emission.[19] It is unlikely that the HNC is due to collisional isomerization induced by collision between vibrationally excited HCN and the other gases, because there is a 35 kcal/mol activation energy barrier between HCN and HNC.[20] This barrier height is larger than the exothermicity of the reaction and hence should be inaccessible.

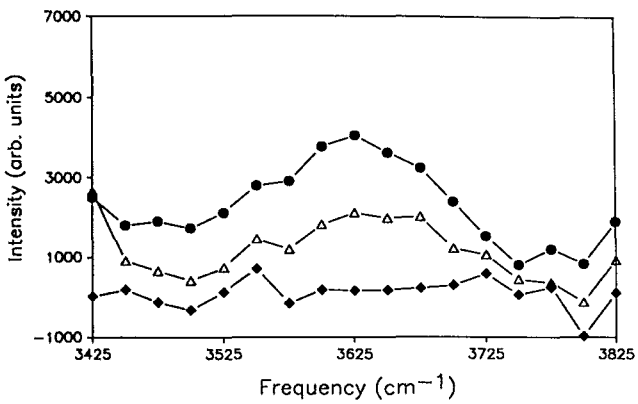

FIG. 8. The infrared emission spectrum of the HNC(011) product from the reaction of CN with C_2H_6. The slit width is 10 mm corresponding to a resolution of about 100 cm^{-1}. The $P_{C_2H_6}$, $P_{C_2N_2}$, and P_{Ar} are 0.077, 1.30, and 9.0 Torr, respectively. The ◆, ●, and Δ are for reaction times of 0, 15, and 35 μs, respectively.

Theoretical studies on the vibrational population of HCN produced in the reaction of CN radicals with hydrocarbons have not been done. There have been theoretical studies of CN reactions with H_2 by both Brooks and Clary, Wagner and Raymond, and Sun and Bowman.[21–23] These studies suggest that the second H atom acts as a spectator and most of the exothermicity goes into the bond that is being formed. Sun and Bowman calculations showed that the bending mode of the HCN should also be excited. If the heavier R radical on the hydrocarbon also acts as a spectator then we would expect to see the kind of vibrational excitation that was observed. The present data, though not conclusive, would support the calculations of Sun and Bowman, since it is likely that we are observing excitation of the bending mode and population inversion.

CONCLUSIONS

The laser induced fluorescence technique has been combined with excimer laser photolysis to determine the temperature dependence of the rate constant for the reaction of CN($v''=0$) with hydrocarbons. A three-parameter Arrhenius plot can be used to fit all of the observed rate constants, however, some of the activation energies are negative. Negative activation energies suggest that a collision complex is formed but the rate constant did not change when the pressure was varied from 20 to 90 Torr. Further time resolved ir emission measurements on the vibrationally excited HCN formed in the reaction showed that in some of the reactions with a negative activation energy a population inversion occurred between HCN(0*n*2) and HCN(0*n*'1).

This article is copyrighted as indicated in the article. Reuse of AIP content is subject to the terms at: http://scitation.aip.org/termsconditions. Downloaded to IP: 130.216.129.208 On: Wed, 17 Dec 2014 02:40:12

Thus if any transient complex is formed it does not live long enough to randomize the energy among all of the vibrational modes of the receding partners, or the coupling between the reaction coordinate and the other oscillators is extremely weak.

ACKNOWLEDGMENTS

We gratefully acknowledge the support of the Department of Energy, Basic Sciences program for funding this work under Grant No. DE-FG05-84ER 13213 and of the National Science Foundation under Grant No. 90-08095. Fida Mohammad also thanks the U.S. Agency for International Development for their support during this project.

[1] X. Li, N. Sayah, and W. M. Jackson, J. Chem. Phys. **81**, 833 (1984).
[2] X. Li, N. Sayah, and W. M. Jackson, J. Chem. Phys. **83**, 616 (1985).
[3] G. E. Bullock and R. Cooper, J. Chem. Soc. Faraday Trans. 1 **68**, 2185 (1972).
[4] X. Li, N. Sayah, J. F. Caballero, and W. M. Jackson, J. Photochem. Photobiol. A **45**, 177 (1988).
[5] R. J. Balla and L. Pasternack, J. Phys. Chem. **91**, 73 (1987).
[6] C. Anastasi and D. U. Hancock, J. Chem. Soc. Faraday Trans. 2 **84**, 9 (1988).
[7] D. A. Lichtin and M. C. Lin, Chem. Phys. **96**, 473 (1985).
[8] J. de Juan, I. W. M. Smith, and B. Veyret, Chem. Phys. Lett. **132**, 108 (1986).
[9] B. Atakan, A. Jacobs, M. Wahl, R. Weller, and J. Wolfrum, Chem. Phys. Lett. **154**, 449 (1989).
[10] Wayne P. Hess, J. L. Durant, and F. P. Tully, J. Phys. Chem. **93**, 6402 (1989).
[11] R. Jeffery and K. H. Castleton, J. Phys. Chem. **95**, 2374 (1991).
[12] M. E. Jenkin and R. A. Cox, J. Phys. Chem. **95**, 3229 (1991).
[13] R. S. Timonen, J. A. Seetula, and D. Gutman, J. Phys. Chem. **95**, 4009 (1991).
[14] J. B. Halpern and W. M. Jackson, J. Phys. Chem. **86**, 973 (1982).
[15] M. M. Maricq, M. A. Smith, C. J. S. M. Simpson, and G. B. Ellison, J. Chem. Phys. **79**, 6154 (1981).
[16] G. Herzberg, *Molecular Spectra and Molecular Structure I, Spectra of Diatomic Molecules*, 2nd ed. (Van Nostrand, New York, 1950).
[17] I. W. M. Smith and J. F. Warr, J. Chem. Soc. Faraday Trans. **87**, 807 (1991).
[18] D. L. Yang, T. Yu, N. S. Wang, M. C. Lin, Spring American Chemical Society, Atlanta Meeting, Physical Chemistry Abstracts, # 235 (1991).
[19] A. G. Maki and R. L. Sams, J. Chem. Phys. **75** 4178 (1981).
[20] P. K. Pearson and H. F. Schaefer III, J. Chem. Phys. **62**, 350 (1975).
[21] A. N. Brooks and D. C. Clary, J. Chem. Phys. **92**, 4178 (1990).
[22] A. F. Wagner and R. A. Bair, Int. J. Chem. Kinet. **18**, 473 (1986).
[23] Q. Sun and J. M. Bowman, J. Chem. Phys. **92**, 5201 (1990).

This article is copyrighted as indicated in the article. Reuse of AIP content is subject to the terms at: http://scitation.aip.org/termsconditions. Downloaded to IP: 130.216.129.208 On: Wed, 17 Dec 2014 02:40:12